Journal of Computational Physics 244 (2013) 264–278

Contents lists available at SciVerse ScienceDirect

Journal of Computational Physics

journal homepage: www.elsevier.com/locate/jcp

An agent based model of integrin clustering: Exploring the role of ligand clustering, integrin homo-oligomerization, integrin–ligand affinity, membrane crowdedness and ligand mobility

Yousef Jamali, Tahereh Jamali, Mohammad R.K. Mofrad *

Molecular Cell Biomechanics Laboratory, Department of Bioengineering, University of California, Berkeley, CA 94720, United States

ARTICLE INFO

Article history:
Available online 29 September 2012

Keywords:
Integrin
Integrin clustering
Focal adhesions
Cellular mechanotransduction
Computational physics
Multiscale
Agent-based modeling

ABSTRACT

Integrins are cell-surface protein heterodimers that coordinate cellular responses to mechanochemical cues from the extracellular matrix (ECM) and stimulate the assembly of small adhesion complexes, which are the initial sites of cell-ECM adhesion. Clustering of integrins is known to mediate signaling through a variety of signal transduction pathways. Yet, the molecular mechanisms of integrin clustering are poorly understood. In this paper, we develop computational models, using agent based modeling (ABM) techniques, to explore two key underlying mechanisms of integrin clustering, namely ligand organization and integrin homo-oligomerization. Our models help to shed light on the potential roles ligand clustering and integrin homo-oligomerization may play in controlling integrin clustering. A potential mechanism for the clustering of integrin is discussed and the effects of other parameters such as integrin–ligand affinity, membrane crowdedness and ligand mobility on integrin clustering are examined.

1. Introduction

Integrins are key plasma membrane sensory molecules that are essential for the cell adhesion to the extracellular matrix (ECM) in multicellular organisms [2,3]. These receptors bind extracellular matrix proteins and help mediate translation of mechanical signals into a cascade of biochemical signals that trigger a wide range of cellular responses [1,8,10]. These molecules show a high propensity to cluster when bound to adhesion ligands [24]. In addition, integrin clustering can be affected by ligand–integrin binding. The importance of ligand binding was established by nonphysiological techniques [4,11]. It has been revealed that integrin clustering is triggered by, or linked to, formation of focal adhesions between the cell and ECM and is required to invoke signal transduction mediated by the integrin. But the precise mechanism of integrin clustering has remained a mystery [15].

Integrins are composed of two non-covalently linked α and β chains (subunits), which form a heterodimer and bind to specific sequences of ligands, with the major one being the tripeptide RGD (Arginine, Glycine, Aspartate) sequence, found in several ECM proteins [22,23,28,30]. Each integrin subunit contains a large extracellular domain with a ligand-binding region, a single-pass transmembrane (TM) spanning domain, and a short cytosolic domain that interacts with cytoskeletal proteins [16,35]. Integrins, while residing in the cell membrane, can shift between three states: inactive, active and clustered. In the resting (inactive) state, integrins exhibit low affinity for ligands [33] and this affinity increases in the active state [7,12,19].

* Corresponding author. Address: Department of Bioengineering, University of California Berkeley, 208A Stanley Hall #1762, Berkeley, CA 94720-1762, United States. Tel.: +1 (510) 643 8165; fax: +1 (510) 642 5835.
E-mail address: mofrad@berkeley.edu (M.R.K. Mofrad).
URL: http://biomechanics.berkeley.edu (M.R.K. Mofrad).

0021-9991/$ - see front matter © 2012 Elsevier Inc. All rights reserved.
http://dx.doi.org/10.1016/j.jcp.2012.09.010

The transmembrane domains of integrin are believed to be close to each other in the inactive state and are separated upon either intracellular elements or ligand binding in the active state. In this state, affinity of the ligand for integrin increases but receptor aggregation does not change. Dissociation of the integrin transmembrane domains facilitates the self-association of these isolated domains to form homodimers and homotrimers with other α and β subunits, respectively [18,20–22,24].

These homo-oligomerization interactions provide a plausible eventuality for integrin clustering and could also help integrin activation by stabilizing the integrin in its activated state [18,20–22,24]. It would be possible that integrin activation can induce integrin to organize in clusters and increase strength of integrin binding integrin valency. Receptor clustering plays an important role in the regulation of adhesion [32] as alterations in integrin clustering may lead to defects in cell adhesions and other biological functions [18]. In addition, integrin clustering can be inferred not only from the presentation of a ligated integrin and affinity between integrin and ligand but also from surface concentrations of ligand and in addition ligand clustering. In fact, many of the ligands that integrins bind are multimeric and have many sites for integrin binding [4,6,13].

A relationship between the number, size and distribution of integrin aggregations in the cell membrane and the concentration of ECM ligands and their affinity for integrins has been revealed [27]. It has been also suggested that properties of the ECM such as ligand chemistry and matrix stiffness can influence integrin clustering and formation of focal adhesions [27].

In this work, we develop agent based modeling (ABM) techniques to simulate the phenomena involved in integrin clustering. The goal of the models presented here is to describe how changes in integrin clustering properties can be associated with key model parameters such as ligand distribution, homo-oligomerization of integrin subunits, membrane crowdedness, the affinity between alpha–alpha subunits and beta–beta subunits, and also affinity between integrin and ligands.

2. Methods: simulating biochemical systems using ABM

Biochemical systems are traditionally modeled using ordinary or partial differential equations. The main assumption in these models is that the system is continuous and deterministic. Neither of these assumptions would truly fit biochemical microsystems, especially that of living cells. The discrete, heterogeneous, random and stochastic nature of biochemical systems, together with the underlying component interactions and geometrical dependency of these interactions decrease the reliability of continuous methods. In particular, randomness and stochasticity cannot be ignored in the cell. Moreover, the number of biochemical species in the cellular system (e.g. signaling proteins) is very small and fluctuations in their concentration are significant. In contrast to differential equation-based methods, the agent-based modeling (ABM) approach has the ability to model the individual molecules and the discrete interactions that take place between them. The aim of ABM is to represent the heterogeneous nature of the system explicitly by modeling each molecule of the real system as an agent. Each agent has different states and exhibits different behaviors based on various environmental conditions. In addition to interactions with the individual agents, ABM considers interactions with the environment, so that each agent can interact with the environment as it moves within it and interacts with other agents. Rather than using reaction rate constants, which would mean ignoring the stochastic behavior of interactions, the ABM technique assigns a certain probability when assessing individual interactions. In other words, ABM uses stochastic reaction constants as a replacement for macroscopic kinetic constants. The behavior of the system will emerge from both the individual behavior of, and the interaction between, the participating agents. The approach in ABM is a bottom-up approach where the rules are simple and local but result in the growth in complexity and completeness of the system's behavior. A major drawback of agent-based models is their computational cost which limits the spatial and temporal resolutions when compared to ODE/PDE methods but still far beyond those achieved by Brownian dynamics simulations. Due to the stochastic nature of the model, the result and emergent behaviors of the system should be averaged over separate independent simulations with the same initial configuration. In general, when an ABM model is built to simulate a certain phenomenon, we need to identify three terms; the agents, environment, and the rules defining how agents interact with each other and with their environment. In this study specifically, the agents are different molecules such as ligand and integrin subunits, the membrane and extracellular medium construct the *in silico* environment, and finally, the movement and the interaction between agents constitute the rules governed by the diffusion and biochemical interaction properties of the biological system. Agents are building blocks of the ABM technique and represent the elements of the actual system. The agents can move and interact with each other and create a complex structure or exhibit complex behaviors. Each agent is characterized by some property and state, for example each agent type in our model has properties such as the volume it occupies, density, movement probability, and binding partners; and each individual agent inherits these properties in addition to other properties such as the position and conformational state.

Generally the agents can be eliminated from, or created in, the system or converted to other agent types. But in our cases, the total running time of the simulation is typically too low to consider the denaturation or elimination of proteins or changes in the concentration based on unrelated signaling pathways and mechanisms. The ABM environment is discretized and divided into a number of cells, which we term each a 'compartment' here for the sake of clarity and to avoid similarity with biological cells. In ABM, it is usually preferred to discretize the space with compartments that are uniform in shape and size. Consequently, we are limited to a few shapes such as triangles, squares, and hexagons in two dimensional spaces, and cubic and rhombic dodecahedron in three dimensions. Each compartment can have properties such as position, maximum volume and viscosity, and each agent distinguishes between compartments via these properties and is directly affected by them. Individual or, in our case, multiple agents can move into an individual compartment if the volume of the agents does not exceed the free volume of the compartment. After discretizing the environment, ABMs can implement a range of

Table 1
Number of binding sites for each agent to attach to other agents.

	Ligand	α subunit	β subunit
Ligand	–	1[b]	
α subunit	–	1[a]	1
β subunit	1	1	2[a]

[a] We suppose that in oligomerization, α subunits can form homo-dimers and β subunits form homo-trimers.
[b] Ligands attach to the position between α and β subunits, in our model ligands can attach to either α or β subunits.

neighborhood types among agents, such as von Neumann, Moore and extended von Neumann. In a particular time step, each agent can interact with a subset of agents that are located within neighboring compartments as well as in the same compartment. This neighborhood can refer to the physical proximity of compartments or other relational connectedness such as the existence of periodic boundary conditions in all or some directions. The last important factor in ABM is the rules that govern changes of the state and properties as a function of the position, time, and the property of neighboring agents. These rules can be divided into two categories: (1) rules that are explicitly independent of other agents, i.e. movement of agents, and (2) rules that consider other agents and interactions with them like binding and activation. These rules should be as simple as possible and mimic what happens locally in the neighborhood of the agent in real systems. A chief issue in the ABM approach of applying these governing rules is the asynchronous occurrence of events, which unlike the real system where all of the agents simultaneously interact with each other and are synchronously transformed to new states, the ABM method applies rules sequentially due to the nature of serial computation. For example, in a biochemical environment, all of the molecules simultaneously move and several of them may collide and possibly interact with each other to create a complex while others dissociate from each other in a synchronous manner. In our simulations, we apply the movement and interaction rules sequentially by choosing a particle and applying the rules and subsequent state changes to it, and afterward selecting the next particle to repeat the process. This can cause some artifacts that can be compensated by performing a random selection method for applying rules to agents.

In the following, we will explain how we attempt to mimic the real system and will set up *in-silico* agents, the environment and rules. To simulate integrin clustering, the model system is constructed using various agents such as ligand (RGD in fixed ligand and tenascin in mobilized one), integrin subunits (α and β subunits), and some inert membrane proteins. The number of each agent type is calculated based on their density and the volume of the simulated environment. We have used their Stokes radius (i.e. the radius of a hard sphere that diffuses at the same rate as the molecule) for calculation of diffusion coefficient. The agents volume was calculated either by dividing their mass by the average density of proteins ($\bar{\rho}_{protein}$: 1.35gr/cm^3) or based on their 3D structure (PDB information) where available. Agents have additional properties such as the ability to move or the agent's current activity state, which are binary properties and switch between on and off. Another important property of agents is the number of available binding sites each agent has for attaching to other agents (Table 1). In our model, we discretize the environment with simple cubic compartments; each cube is assigned an environmental property, differentiating whether it is part of the membrane or extracellular environment. The cell membrane is assumed to be flat against the extracellular matrix, the environment is composed of two layers, a two-dimensional lattice representing the cell membrane and another one which is in contact with the membrane and represents the extracellular matrix. In some case studies, e.g. when exploring the effect of ligand mobility, the second layer is extended to a 3D environment to mimic the extracellular environment in which ligand is soluble. The size of the membrane is 1 μm^2 and composed of 100×100 compartments with periodic boundary conditions in the X and Y direction (parallel to the membrane).

Two important rule sets are applied in each time step, one is related to the agent movement and the other is for interactions. In order to accurately model diffusion of the agent, each agent can move from one compartment to its neighbors with a probability proportional to its diffusion coefficient. Agents in three dimensions (e.g. ligands in free extracellular space) have 6 neighbors and agents which are embedded in two dimensions (e.g. integrin subunits in the membrane) have four possible neighboring compartments to move to. After randomly selecting a neighboring compartment, the agent can move to the new location with a probability p_m:

$$p_m = p_D p_v \tag{1}$$

where p_D is the probability related to diffusion coefficient of the molecule and p_v is the probability related to the crowdedness and is a function of free space in the destination compartment. We can show that for p_D we have

$$p_D = \frac{2DN_{Dim}\Delta t}{N_{Neb}(\Delta L)^2} \qquad \Delta t \to 0 \tag{2}$$

N_{Dim} is the space dimension number. ΔL is the distance between the center of two neighboring compartments, N_{Neb} is the number of neighboring compartments, and Δt is the simulation time step, which should be significantly small. D is the diffusion coefficient of the molecules, which is a function of size and the viscosity and temperature of the medium. For diffusion of particles through a medium with low Reynolds number, the Einstein–Stokes equation holds:

Table 2
The kinetic off rates and dissociation equilibrium constants used in the present simulations.

	k_{off}	k_d	Ref.
Integrin–ligand	0.072 s^{-1}	0.4 μM	[9,22]
Alpha dimer	Estimated	288 μM	[20]
Beta trimer	Estimated	131 μM	[20]

$$D = \frac{k_B T}{6\pi\eta r} \tag{3}$$

where k_B is Boltzmann's constant, T is the temperature, η is the environment viscosity, and r is the Stokes radius of the particle. It must be mentioned that the value of Stokes radius of the agents are gathered from different references and is the input of the simulation for calculation of the diffusion coefficient.

For p_v we have

$$p_v = \max\left(\frac{V_c - V_0}{V_c}, 0\right) \tag{4}$$

V_c is the volume of the cell, and V_0 is the occupied volume. This part represents the crowdedness and reflects the fact that in a crowded system the diffusion of the particle is decreased. As previously mentioned, the second major rule set is interaction between agents, which is governed by an agent's available binding sites and its neighboring agents. Suppose agent A has one binding site to attach to agent B with an association constant of k_{on} and a dissociation constant k_{off}. In each time step, if agent A has an empty binding site, it checks for agent B in its neighboring compartments (and nested compartment in the case of multiple agents occupying a single compartment). If it finds a molecule of agent type B with an empty binding site to A, the agent A will be attached to agent B with a probability of p_{on}, creating a complex that will diffuse through the environment. If one of them is a fixed molecule, e.g. a tethered ligand, the complex will be immobilized. As the complex moves, each underlying component can move as long as it does not detach from molecules it is bound to. Similarly, in each time step, each of the bound molecules that make up a complex can be dissociated from the complex with a probability of p_{off}. The relations between kinetic constant and the probability of attachment/detachment are:

$$\begin{aligned} p_{off} &= k_{off}\Delta t \\ p_{on} &= \frac{k_{on}\Delta t}{SV_c(N_{Neb} + \alpha)N_A} \end{aligned} \tag{5}$$

In these equations, S is 1 if A is a different type of molecule from B and 2 if both agents are identical. N_A is the Avogadro's number. We should emphasize that this relationship is valid only if the experimental value of k_{on} and k_{off} are obtained in low concentrations of the reactants. The values of kinetic constants that we used in our simulation are summarized in Table 2.

In this work, we denote integrin molecules as a cluster if (i) they are in the neighborhood of each other, (ii) all activated integrins are attached to ligands, and (iii) the total number of integrins is more than two. The simulation is typically run for 5 min. We let the system reach equilibrium, typically within 2 min, and then start the sampling following equilibration. Each 2 s we sample the system, and finally we average over them.

3. Results and discussion

3.1. Effects of ligand distribution on integrin clustering

First we explore the ligand clusters, which we refer to as ligand islands here forth, and the role of ligand island parameters on the clustering of integrins. To create the ligand islands, we tethered the ligands together in a square geometry. For simplicity, these islands were distributed uniformly through the ECM with a local density of 170 nmol/m^2 (10^5 μm^{-2}) as shown in Fig. 1. The average concentration of ligands ([*Ligand*]) were varied from 1.6 nmol/m^2 to 16.6 nmol/m^2 (1000 to 10000 μm^{-2}). The size of ligand islands were varied from 100 to 10000 nm^2. The concentration of integrins, i.e. α–β subunits, ([*Integrin*]) was varied from 0.17 nmol/m^2 to 8.5 nmol/m^2 (100 to 5000 μm^{-2}) [4,13,31]. In all of the graphs, the unit of the integrin cluster size is 100 nm^2, i.e. the range of average size of the integrin clusters varies from 0 to 10 000 nm^2.

As shown in Fig. 2, when the size of ligand islands decreases, the size of integrin cluster reduces with a constant rate. In other words, there is a linear relationship between the ligand islands size and integrin cluster size; the slope depends on the concentration of ligand and integrin. However at very low concentrations of integrin, the ligand island's size has no significant effect on integrin clustering.

Comparing different surfaces in Fig. 2 suggests that the average size of integrin clusters increases as the concentration of integrins increases. At a given integrin concentration, considering a fixed number of ligand islands, increasing the size of the ligand islands would lead to formation of larger integrin clusters (see Fig. 3). However, at some integrin concentrations, there is a maximum achievable integrin cluster size, and interestingly, ligand islands larger than these optimal sizes have a

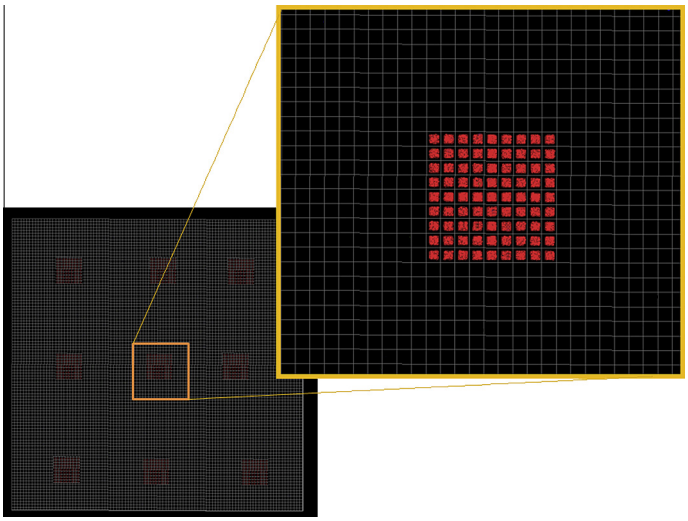

Fig. 1. Enhanced view of a single ligand island in ABM space. Red molecules represent the ligand. (For interpretation of the references to colour in this figure legend, the reader is referred to the web version of this article.)

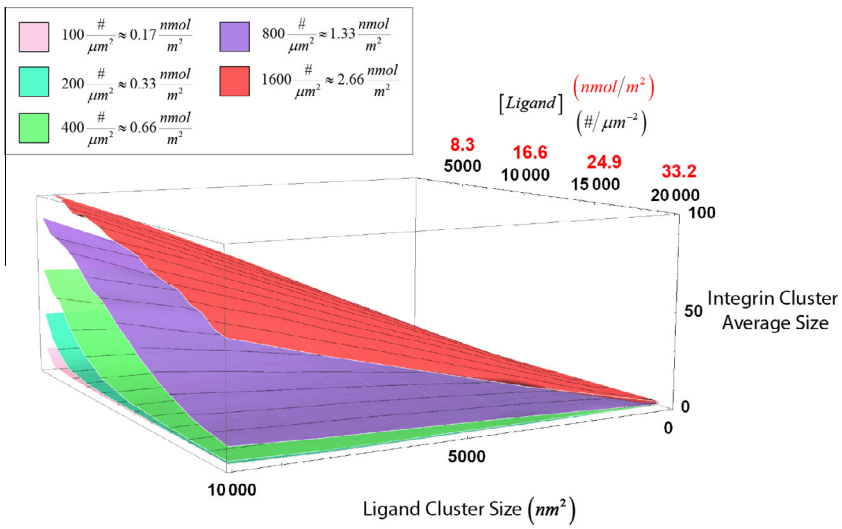

Fig. 2. The role of ligand cluster size and ligand concentration on integrin cluster size. Each surface is related to a specific integrin concentration.

negative effect on integrin clustering. By decreasing the number of ligand islands, the average size of integrin clusters increases. In addition, the results show that at smaller ligand island sizes, the role of integrin concentration is less significant (surfaces are nearer to each other than at larger ligand island sizes). Based on the results presented here, it can be speculated that the largest integrin clusters will require the existence of a small number of large ligand islands. In this scenario, if the size and number of ligand islands are decreased and increased, respectively, the size of the integrin cluster will be reduced. These results are consistent with the experimental evidence that shows integrin clustering requires a high density of local ligand in the extracellular environment. In fact, it has been shown that most ligands are multimeric [4,6,13,29] and integrin clustering increases while the ligand island size is larger [17,25]. In addition, the experimental evidence confirms our results and shows that lower concentrations of ligand islands increases the integrin cluster size [34].

We hypothesize that this phenomenon may result from a competition scenario, i.e. by decreasing the ligand island concentration, the chance of attachment to the remaining ligand islands will be increased, and consequently the total number of integrins in each cluster will be increased. However by decreasing the size of ligand islands, the accessible surface available for formation of integrin clusters will be limited, which leads to a reduction in the average size of integrin clusters. Regarding the maximum value and biphasic behavior of integrin cluster size in the second region, as shown in Fig. 3, when the size of the ligand islands are small, the size of the integrin cluster will be limited to the size of the ligand islands. However, because

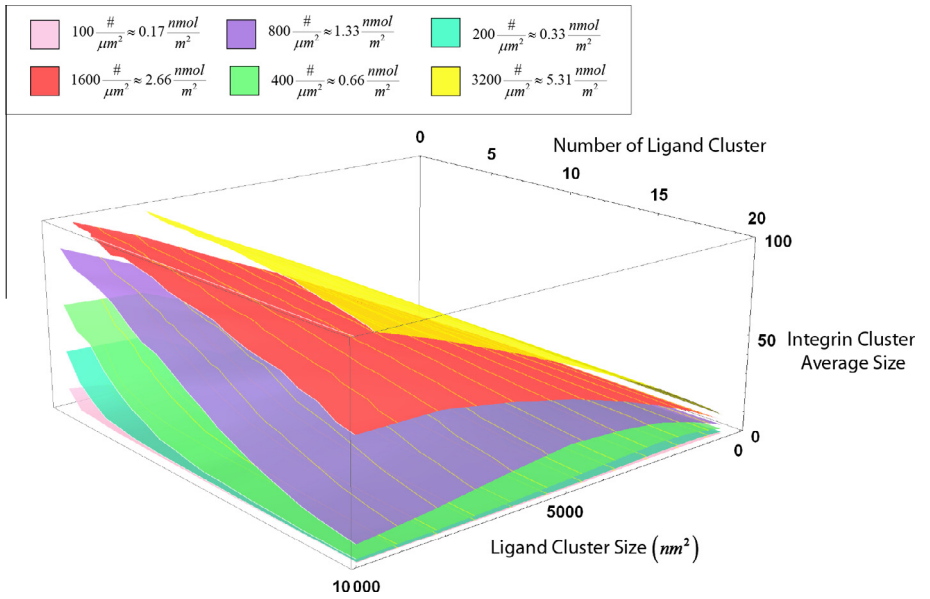

Fig. 3. The role of ligand cluster size as well as number of ligand islands on integrin cluster size. Each surface is related to a specific integrin density.

the number of integrins in the system is constant, by increasing the size of the islands, most of the integrin will be bound to ligands and no further integrin remains to assist in increasing the size of the integrin clusters. Following this, by increasing the size of the ligand island, the competition between ligands will be increased which leads to the formation of more than one small integrin cluster in each ligand island. Hence, the average size of integrin cluster will be decreased.

Regarding the number of integrin clusters as shown in Fig. 12, there is an inverse correlation between the number and the size of integrin clusters. We can assume that the geometrical average of size and number of clusters is constant; however, there is a reduction in the geometrical average at low numbers of ligand islands.

3.2. The effect of homo-oligomerization on integrin clustering

Here we explore the effect of homo-oligomerization of the integrin subunits on integrin clustering. In order to test the effects of homo-oligomerization, the ligands were tethered randomly and the density was varied from 1.6 nmol/m^2 to 33.2 nmol/m^2 (1000–20,000 μm^{-2}), and the integrin density was varied from 0.17 nmol/m^2 to 5.44 nmol/m^2 (100–3200 μm^{-2}). We ran four groups of simulations with varied affinities between subunits which consisted of no affinity between subunits, the experimentally reported affinity [20], and also with higher affinities, i.e. two and four units more than the *in vitro* value.

In Fig. 4 each surface is fit to 100 calculated points via bicubic interpolation. Each point corresponds to a simulation at a fixed ligand and integrin density. The total simulation time was 4 min. The first 2 min of the simulation was carried out for equilibration and the sampling was done during the next 2 min.

The results of varying the affinity between subunits on integrin clustering are shown in Fig. 4. Regarding the homo-oligomerization processes, comparing different surfaces shows that increasing affinity between homo-subunits enhances the size of integrin clusters. The relation between affinity and the average size of integrin clusters is not linear and depends on the concentration of ligand and integrins. By comparing the blue[1] and red surfaces in Fig. 4, at some points the ratio of the size of integrin clusters can exceed 9 while at other points the ratio is less than 1.2. The greatest impact of affinity on integrin clustering is seen when the ligand and integrin concentrations are near low and high, respectively. Another interesting result arises when surfaces with the *in vitro* affinity and without affinity are compared. The difference in integrin clustering between the two configurations is negligible (the yellow surface is hidden by the blue surface at this resolution), confirming that the reported *in vitro*, value does not significantly affect integrin clustering in these conditions. In order for the affinity between homo-subunits to play a significant role in integrin clustering, the value of this affinity needs to be greater than what has been measured *in vitro*. We should mention that, to the best of our knowledge, this is the only reported affinity value and according to the authors, this value is calculated based on the study in phospholipid micelles [20] and the *in vivo* value is expected to be higher.

Generally speaking, it seems that when ligands are tethered and immobilized, the effect of homo-subunit affinity on integrin clustering is lower compared to the role of the ligand clustering. Hence we could speculate that appropriately clustered

[1] For interpretation of color in Figs. 4, 9 and 11 the reader is referred to the web version of this article.

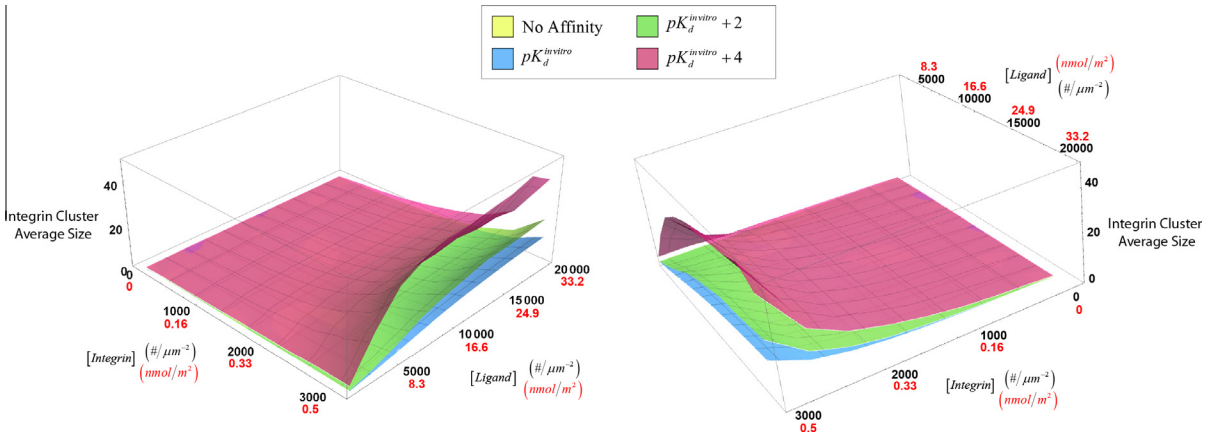

Fig. 4. The effect of affinity between subunits on integrin clustering.

ligands play the main role in the formation of the integrin clusters as an initial step to forming focal adhesion. However as the results show, the homo-oligomerization has a positive effect on integrin clustering. Additionally, some experimental results have shown that homomeric association of the transmembrane domains leads to integrin clustering. Homo-oligomerization provides a mechanism for inducing the formation of integrin clusters [36] as the α and β subunits readily participate in homophilic association leading to the formation of homodimers and homotrimers, respectively. Moreover, it has been revealed that blocking integrin dimerization decreases integrin clustering. Additionally, on-lattice Monte Carlo simulations have shown that integrin dimerization can produce integrin clustering [4,5]. Hence, part of the focus of this paper has been on homo-oligomerization of integrin subunits.

It seems that ligand and integrin concentrations affect the size of the integrin cluster independently, hence the size of the integrin cluster can be considered as a multiplication of two functions, one depending on the integrin concentration, the other depending on the ligand concentration. By fitting different curves, it seems that at a fixed ligand concentration, the integrin cluster size increases exponentially when the integrin concentration increases:

$$\bar{S}_{Int\,Clsr} \propto a(\rho_{Int})^n \tag{6}$$

with α and n being positive constant numbers and n being greater than one. This is not surprising considering that by increasing the number of integrins we expect more integrins to be attached to the ligand while the number of integrin–ligand complexes will be increased at the contact area of the cell membrane. Subsequently, each individual integrin–ligand complex has a higher chance to find other complexes near itself. As a result, with the connection of these neighbors the system will have larger integrin clusters. On the other hand with a fixed concentration of integrin, the growth of integrin clusters as functions of ligand islands can be approximated as:

$$\bar{S}_{Int\,Clsr} \propto \frac{b\rho_{Lig}}{1+c\rho_{Lig}} \tag{7}$$

where b and c are constants. It is clear that for integrin clusters to form proximity of multimeric ligands is essential. At a very low concentration of ligands (with a random configuration), there is a low probability that two ligands neighbor each other and this property is a limiting factor in integrin clustering and hence the integrin cluster size is highly dependent on the ligand concentration. Hence, as other theoretical results show [4], by increasing the ligand concentration, the size of integrin clusters is increased.

However, after a certain point, the entire surface will be covered with ligands, after which the ligand concentration will no longer be the governing factor. Combining Eqs. (6) and (7) we have:

$$\bar{S}_{Int\,Clsr} \propto \left(\frac{b\rho_{Lig}}{1+c\rho_{Lig}}\right)(a(\rho_{Int})^n) \tag{8}$$

Typically, in experiments, the affinity and kinetic constants are calculated in very simple conditions that may be far from *in vivo* settings, and fail to capture the effect of phenomena that modify the interaction of two molecules and the equilibrium concentration of a binding complex. For example, the distribution of molecules, activity of molecules and system crowdedness can alter the direction of a reaction and affect the equilibrium concentrations. In the case of integrin homo-subunits, for instance, in order to investigate the affinity between two α subunits, the subunits are left free to actively interact with each other in the experimental environment in absence of β subunits. However, the *in vivo* scenario is slightly different; α subunits in conjunction with β subunits form an integrin molecule, which, as a first step, would attache to the ligand. After the attachment, for example, the α subunits will be activated to interact with other activated homosubunits. Since the activated

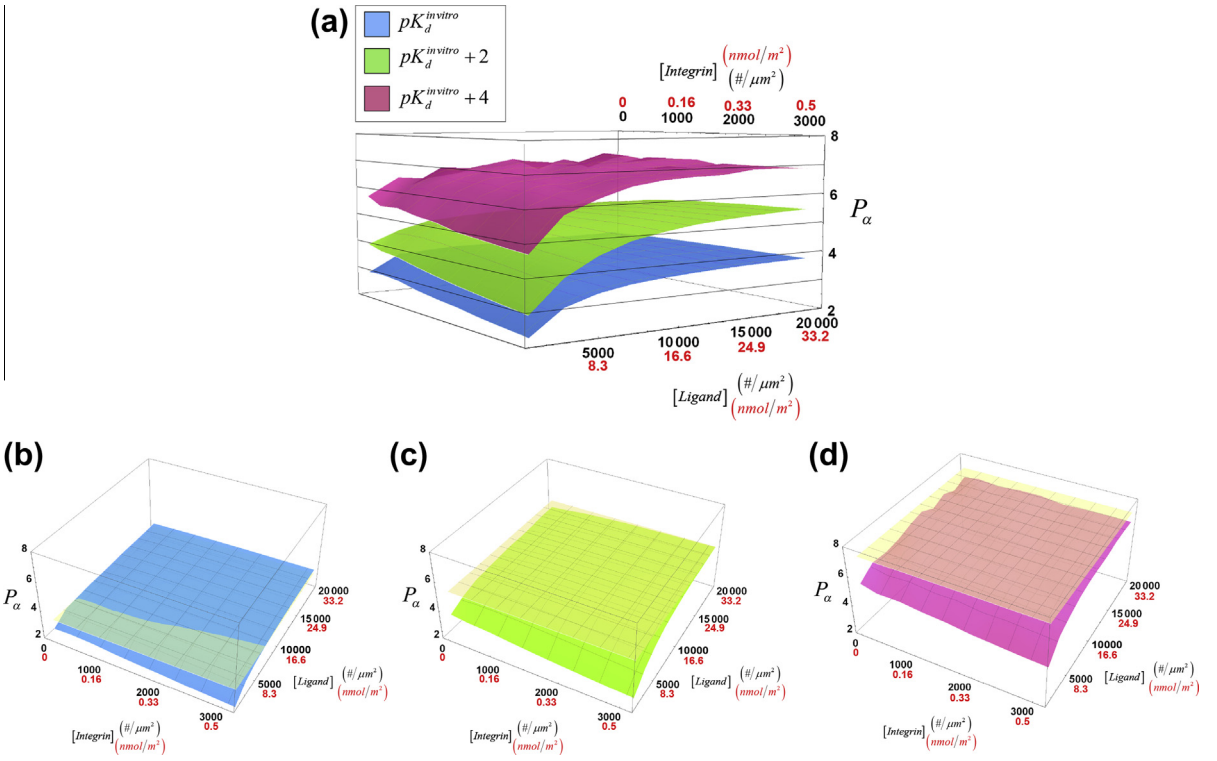

Fig. 5. The effective affinity as a function of integrin and ligand density. (a) Each surface is related to the specific affinity which has been used as input for the simulations. (b)–(d) effective affinity is compared with the affinity which has been used as input for the simulations (yellow surface). (For interpretation of the references to colour in this figure legend, the reader is referred to the web version of this article.)

subunits are attached to immobilized ligands, they have a small degree of freedom to search the space for other activated α subunits. All of these circumstances change the final number of α homodimers when compared to *in vitro* results. In order to investigate these effects we have defined a new parameter, termed the 'effective affinity' between α subunits, P_α:

$$P_\alpha = -\log\left(\frac{[\alpha]^2}{[\alpha_2]}\right) \tag{9}$$

where $[\alpha]$ is the α subunit concentration and $[\alpha_2]$ is the concentration of jointed α subunits. This effective affinity is dependent on the density of integrin and ligands. Fig. 5 shows the value of effective affinity as a function of integrin and ligand density.

The main observation which is highlighted in the results is the variation and dependency of effective affinity on concentration of ligands and integrins. The minimum value of effective affinity is at the minimum ligand and maximum integrin concentration. The concentration of ligands plays a role as the governing factor. There is a positive relation between the ligand density and effective affinity, that is it can be seen that the effective affinity increases *with the increased ligand density*. However, the effective affinity has an asymptotic behavior and in a high ligand density its value changes slightly. At higher ligand concentrations, effective affinity is independent of the integrin concentration. However, at low concentrations of ligands, the number of integrins has a adverse effect on the effective affinity. This behavior arises due to the fact that when the ligand number is low, there is a limited number of integrins able to attach to the ligand; in addition, the chance for activated α subunits to find each other is low. By increasing the number of integrins, the ratio of the free α and activated α subunits increases and consequently, the effective affinity will decrease. In general, the concentration of ligands has a positive effect on the effective affinity.

In Fig. 5 (panels (b)–(d)), the effective affinity is compared with the affinity that was used as input for the simulations (P_{kd}). The effective affinity has a close relationship with the experimentally measured affinity ($pK_d^{in\text{-}vitro}$) [20] but is dependent on the concentration of integrins and ligands in the system. When $P_{kd} = pK_d^{in\text{-}vitro} + 2$ (Fig. 5(c)), the effective affinity is lower than the input affinity, P_{kd}, and the difference increases as the input affinity increases (Fig. 5(d)). At lower affinities, i.e. $P_{kd} = pK_d^{in-vitro}$ (Fig. 5(b)), in some regions (specifically where ligands are in high concentrations) the effective affinity is higher than the experimentally measured affinity. This shows the biphasic role of ligands. As previously mentioned, the activation of α subunits via attachment to the ligands and therefore the number of ligands is a limiting factor on the formation of α homodimers. However, after formation of a homodimer, immobilization of ligands which are in contact with the subunits

helps to increase the chance of attachment by reducing the diffusion of α subunits and increasing the local density of α subunits, exhibiting both a negative and positive effect on the formation of homodimers. Typically, the negative effect is dominant, however, by increasing the ligand concentration, the negative effect is reduced and the positive effect becomes dominant. For instance, in Fig. 5(b), at a high concentration of ligands, the positive effect is dominant and consequently the effective affinity is higher than the experimentally reported affinity.

3.3. The effect of crowdedness

Membrane proteins make up about 30 percent of the proteins in an organism and 50 percent of the membrane composition [26]. They have various functions resulting from their chemical and physical interactions. To shed light on the effect of membrane crowdedness of other proteins on integrin clustering, we defined a new inert particle type and added it to the *in silico* membrane—the term inert implies that no chemical interactions exist among these particles with themselves nor with other particles. The inert particles represent typical membrane proteins. In the present simulations, the effect of different concentrations and diffusion coefficients of the inert particles on integrin clustering have been taken into account (Fig. 6). The concentration of integrin and ligand in all simulations is kept constant and equal to 1.33 and 16 nmol/m^2, respectively. The concentration of inert particles was varied up to 12 nmol/m^2 (7000 mm^{-2}). Each simulation was run with two different distribution patterns for the ligand, the random configuration (Fig. 6, panels (b) and (d)), and the ordered cluster configuration (Fig. 6, panels (a) and (c)). Each curve is related to a specific inert particle diffusion coefficient. The legend values refer to the ratio of inert particle diffusion coefficient to integrin particle diffusion coefficient. Fig. 6 shows the size of integrin clusters versus the density of particles. Each curve is related to the specific diffusion coefficient of particles. For simplicity all the particles are given the same properties, e.g. volume and diffusion coefficient. The legend shows the ratio of the particle diffusion coefficient to the integrin diffusion coefficient. When the ligand distribution is random (Fig. 6(a)), the effect of inert particles is negligible at the low concentrations. By increasing the crowdedness, especially at lower diffusion coefficients, a phase transition in the size of integrins can be seen, i.e. beyond a certain particle concentration ($[P]_c$), the size of integrin clusters begins to reduce or increase. At low diffusion coefficients this transition happens sooner compared to high diffusion coefficients. There are many factors that may influence the size of integrin clusters, and the inert particle concentration is

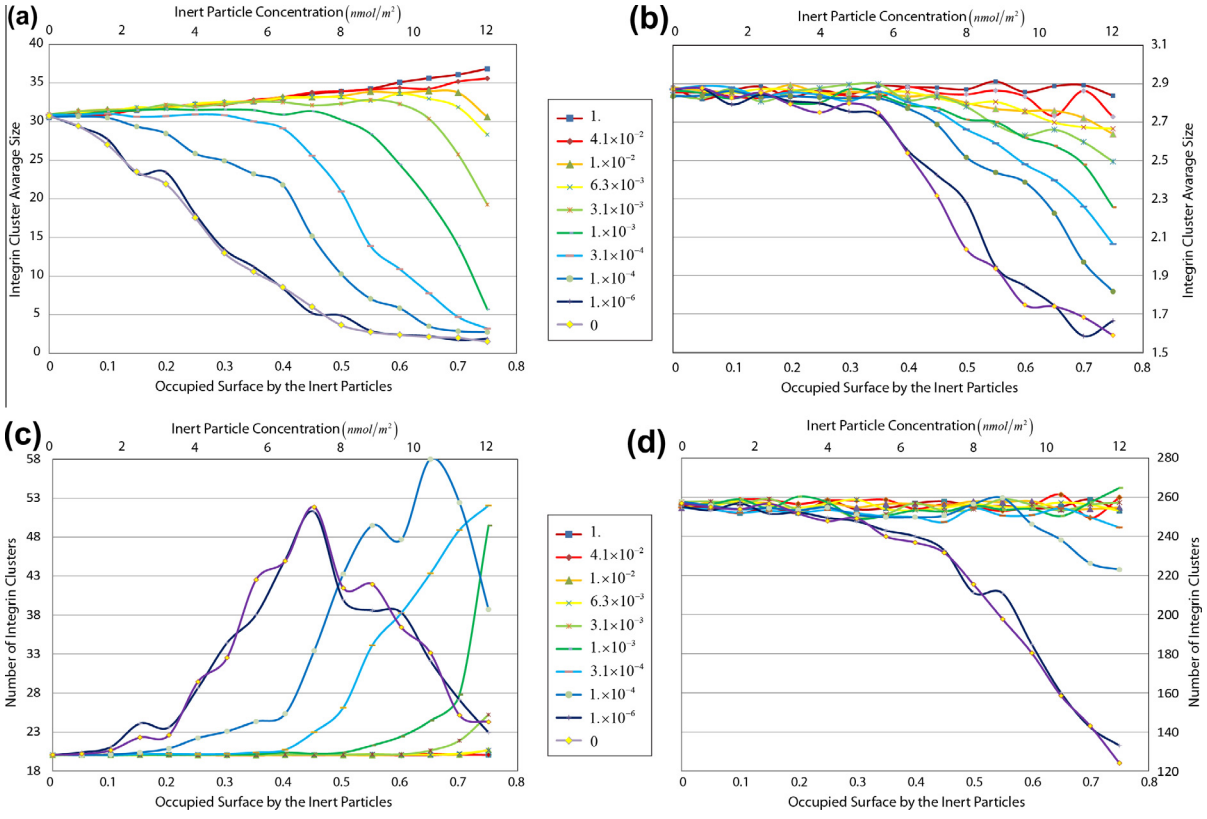

Fig. 6. The effect of membrane crowdedness on integrin clustering. A new inert particle type was defined and added to the in-silico membrane. In the present simulations, the effects of concentration and diffusion coefficient of the inert particles on integrin clustering have been explored. Left and right graphs are the result of simulation with the cluster configuration and random distribution of ligands, respectively.

one of them. It is likely that at low concentrations, other parameters are dominant, but beyond a certain concentration, inert particle concentration becomes a dominant factor and leads to a decrease in the size of the integrin clusters.

When two integrins are bound together, as long as they have affinity for one another and are bound to the ligands, other particles have no effect on them. However, when they are near one another and are not yet bound, the presence of a third particle between them interferes with their interaction and hinders binding of integrins. Hence by increasing the concentration of inert particles the probability of the inert particle interfering is increased and the negative effect of inert particles emerges. Therefore, as the concentration of inert particles increases, the average size of integrin clusters decreases (see Fig. 6). Another reason for this behavior is that by increasing the number of particles, their presence between and around a formed complex tends to increase. This causes a steric repulsion for other integrins, inhibiting their ability to move into proximity of and attach to ligands and could also hinder binding of neighboring complexes to form a bigger complex. However, surprisingly, at high diffusion coefficients of inert particles, increasing crowdedness enhances the integrin cluster size. The underlying mechanism behind this behavior is that at high diffusion coefficients the dwell time of each particle between integrins and complexes is low. Hence, as a result of the high mobility, they move away from the complex and their position is made available for other integrins. In this situation, increasing the number of inert particles results in an increase in the local concentration of integrins due to a reduction of the free space, i.e. the concentration of integrins is artificially increased and subsequently a larger integrin cluster is formed. In general, the effect of inert particles is higher for randomly distributed ligands compared to clustered ligands.

3.4. Effect of the affinity between α-α subunits and β-β subunits

To examine the effect of affinity between homo subunits α–α as well as β–β on integrin clustering, we performed a set of simulations in which we varied subunit affinities at different integrin concentrations. Each surface in Fig. 7 represents the size of the integrin cluster at a fixed concentration of integrin when the affinity between α–α and β–β is changed independently. k_0 is the *in vitro* dissociation constant that has a different value for each type of the homomers. Varying the affinity for each homomer begins from an *in vitro* value and is increased up to 4 units. As the graph shows, the affinity between homo-subunits has a positive effect on the size of integrin clustering. In other words, the size of integrin clusters is enhanced by increasing the affinity of each type of subunit. However, when looking at the direction of the α–α subunit affinity axis (see Fig. 8, red curves), independent of the β–β affinity, three different sub-regions can be distinguished for each curve. In the first sub-region (between $-\log(k/k_0) = 0$ and 1), there is no significant dependency between the affinity and size of integrin cluster and therefore the effect of affinity on integrin clustering is negligible. In fact, in this region the value of affinity is very low and its role on integrin clustering is minimal. Following this, in the second region (between $-\log(k/k_0) = 1$ and 2.5), α–α affinity plays a significant role in integrin clustering size as the increasing affinity of these subunits results in the formation of larger integrin clusters. Generally, two reasons could be suggested for this positive effect. It could be that increased affinity helps integrin–ligand complexes find each other more easily in less time, and as a result, the initial clusters become larger. In the second region, due to binding of integrins via their homo-subunits, the clusters are more stable, leading to a longer cluster lifetime. In the third region (greater than 3), again the size of integrin clusters is fairly independent of the α subunit affinity. One reason behind this independent behavior could be other parameters that play a limiting role. These parameters regulate the upper limit of integrin clusters and prevent further increase in the integrin cluster size by increasing the

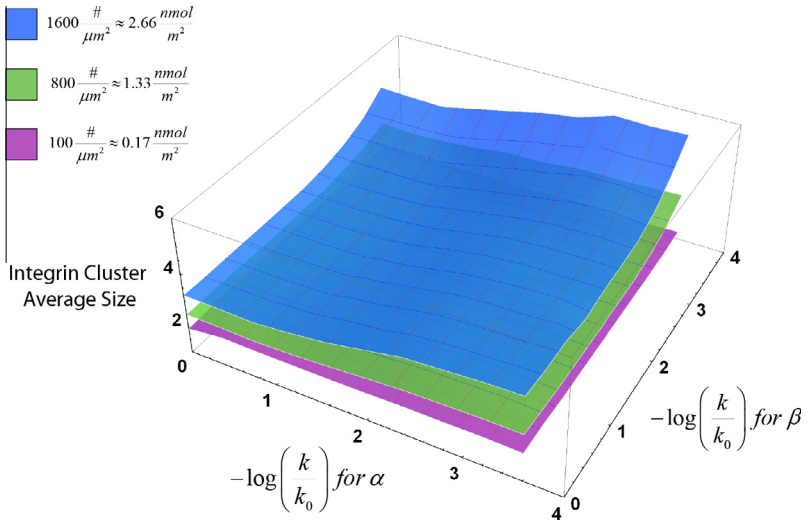

Fig. 7. The effect of integrin homo subunits affinity. Surfaces represent the size of the integrin cluster at a fixed concentration of integrin when the affinity between α–α and β–β is changed independently.

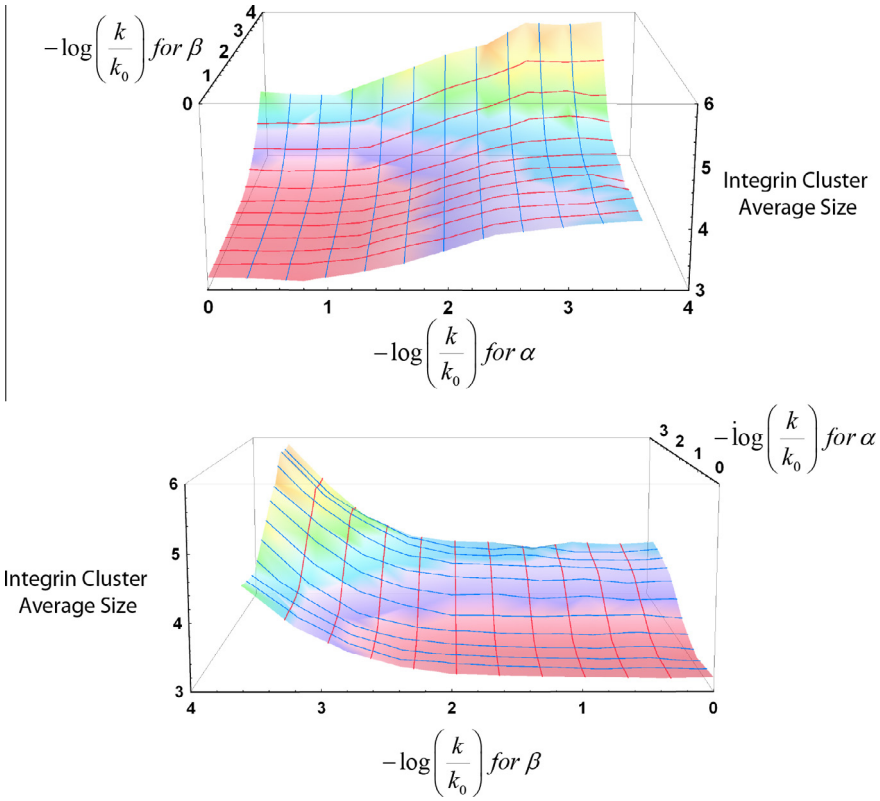

Fig. 8. Effect of integrin homo subunits affinity on size of the integrin cluster at a fixed concentration of integrin (2.66 nM/m^2). Red and blue curves are the integrin clustering size at the fixed β–β and α–α affinities, respectively. (For interpretation of the references to colour in this figure legend, the reader is referred to the web version of this article.)

α–α affinity. A similar trend can be found in how the variation in β–β subunit affinity affects integrin clustering (see the blue curves in the Fig. 8(b)). Hence, we expect that by further increasing the β–β affinity, a third region will emerge in the graph.

3.5. Effect of the affinity between the integrin and ligands

The role of the affinity between ligand and integrin in integrin clustering is eamined here. The simulations were carried out in two different distribution patterns of ligands: clustered (Fig. 9(a)) and random distribution (Fig. 9(b)). The effect of integrin–ligand affinity was investigated under three different integrin concentrations, namely 0.17 nmol/m^2 (blue curves), 0.85 nmol/m^2 (red curves) and 3.4 nmol/m^2 (green curves). While the affinity between integrin homo-subunits is accounted for in these simulations, our results suggest that this affinity does not affect the general behavior of integrin clustering significantly.

Simulations were carried out for a relatively wide range of physiological ligand affinities. As the results show, our model predicts that when the affinity between the integrin and ligand increases to a terminal value, the size of integrin clusters increases. This terminal value of affinity depends on the integrin concentration and ligand distribution pattern. This behavior is not surprising, considering that increasing the affinity results in an increase in the number of integrin–ligand complexes. Subsequently, the size and the number of the clusters increase. In the graph, after a jump, the curves finally reach a maximum value (see Fig. 9). We denote this region as the saturation phase due to the fact that in this region most of the integrins are bound to the ligand and further increases in affinity would not change the number of bound integrins significantly. It can therefore, be concluded that for each concentration of integrins, there is an optimum affinity (inflection point in the graphs, see Fig. 9) and interestingly, the experimental value (i.e. zero in the horizontal axis) is near the optimum value for many concentrations. Beyond this optimum value, increasing the affinity does not affect the integrin clustering in a significant manner. It could be therefore speculated that the binding affinity between integrin and ligands has been may be evolutionarily optimized.

The clustered configuration significantly enhances the effect of integrin–ligand affinity on the integrin cluster size. Also, the system is more responsive to affinity at a higher density of integrins compared to lower ones. In Fig. 9 (see panels (c) and (d)), the number of integrin clusters under the same conditions is plotted. Interestingly, the number of integrin clusters

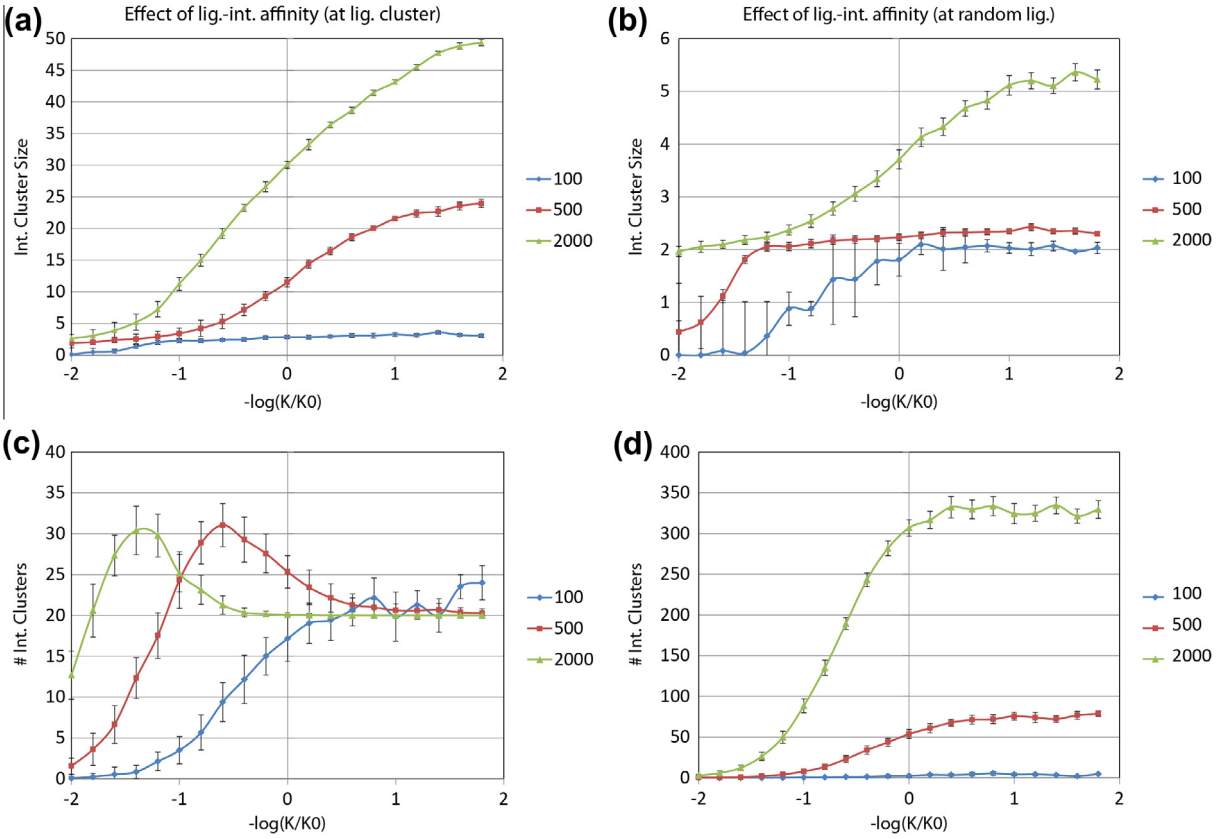

Fig. 9. The role of the affinity between ligand and integrin in integrin clustering. The simulations were carried out with two different distribution patterns of ligands, random (right) and clustered (left). In panels (c) and (d) the number of integrin clusters under the same conditions is plotted.

follows two different qualitative trends based on the ligand distribution pattern. Further examination of the experimental and analytical data explains that variation in integrin binding affinity for ligands is effective for the quantitative modulation of adhesion strength and increasing integrin clusters [14].

3.6. Effect of ligand mobility

Thus far we supposed that the ligands are tethered to substrate and are immobilized. To probe the role of ligand mobility, while varying ligand and integrin concentrations, we performed a set of simulations in which ligands are free to diffuse on the substrate. Our primary aim here is to compare mobile ligands with immobile ligands without the addition of other compounding factors, therefore the diffusion of ligands is limited to movement in a two dimensional surface to avoid introducing effects associated with the movement in three dimensional space. Fig. 10 shows the size of integrin clustering at different concentrations when the ligands are free to diffuse (blue surface) and when the ligands are tethered to the substrate (yellow surface). Our results (Fig. 10(a)) suggest that, as long as there is no affinity between homo-subunits, mobility of the ligand has no significant effect on the size and number of integrin clusters. Movements of ligands do not affect their average statistical distribution and hence the integrin cluster does not change either. It can be expected that the number and size of integrin clusters is independent of diffusion coefficient of either ligands or integrins. However, this is not the case for the affinity between homo-subunits. In this case, as Fig. 10(b) shows, diffusion of ligand improves the integrin cluster size when the integrin subunits have affinity to their homologs. When the ligand is fixed, movement of active subunits is very limited to the proximity the ligand of it is bound to. Hence, the chance for finding other homo subunits is limited to a restricted region around the fixed ligand. On the other hand, when the ligands diffuse, the movement of ligand–integrin complex helps active subunits to explore a larger space and search for homologs to interact with, increasing the chance of homo-oligomerization of active subunits and subsequently, the formation of larger integrin clusters in the system. In two regions of the surfaces in Fig. 10(b), the effect of ligand mobility is high: region of high concentrations of integrin and ligand and region of low concentrations of integrin and ligands. Surprisingly, it can be seen that when one of the components (ligand or integrin) is at high concentrations and the other is at low concentrations, the effect of mobility decreases. In general we can speculate that when the ligands are able to diffuse, the affinity between integrin subunits plays an important role on integrin clustering.

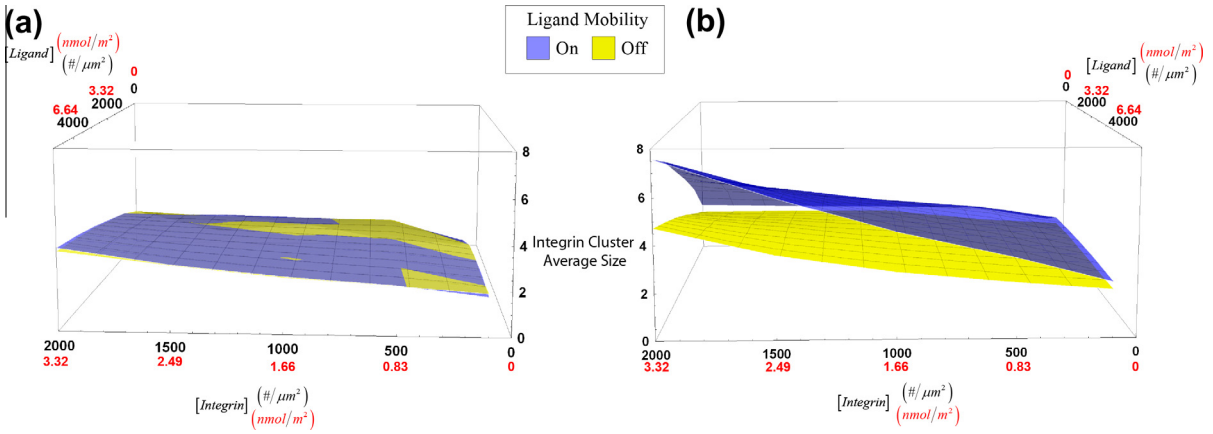

Fig. 10. Effect of ligand mobility. The size of integrin clustering at different concentrations when the ligands are free to diffuse (violet surface) and when the ligands are tethered to the substrate (green surface). (a) No affinity between the integrin homo subunits (b) With affinity between the integrin homo subunits. (For interpretation of the references to colour in this figure legend, the reader is referred to the web version of this article.).

3.7. Ligand diffusion in 3D

Our simulations so far restricted the ligands to only diffuse on the substrate since our aim was to compare the effect of mobility with other results involving integrin clustering on a surface. However, it is obvious that diffusion of ligands is typically in aqueous environments. In other words, the ligand diffuses freely in a three dimensional environment and interacts with the membrane integrins that are in contact with the solution. One of the examples of this type of interaction is the ligand–receptor interaction. When considering the ligand-receptors, the number of ligands is typically much lower than substrate ligand.

We set up the simulations with a cubic ligand container which is in contact with the membrane on one face and has periodic boundary conditions on the other four faces. Fig. 11 presents the results for two conditions: first, when there is affinity between integrins (green surface) and second, when there is no interaction between integrins (red surface). The computed results demonstrate that the size of integrin clusters increases while the concentration of ligand and/or integrin is increased. However, after reaching a terminal concentration (0.85 nmol/m^2 for integrin and 2.55 nmol/m^2 for ligand), the integrin cluster size reaches a maximum and does not grow any larger. These graphs clearly demonstrate that affinity between integrin homo-subunits has a positive effect on integrin clustering. Interestingly, at low concentrations of ligand (Fig. 11 right) there is no integrin clustering in absence of affinity between integrins. This shows that at low concentrations of soluble ligands, the affinity between integrins plays an important role in integrin clustering. Fig. 11 shows the impotency of integrin homo-subunit interaction at low concentrations of soluble ligands. It seems that at low concentrations of *soluble ligands*, the role of integrin–integrin (receptor–receptor) interactions on integrin clustering is vital and without such interactions the integrin

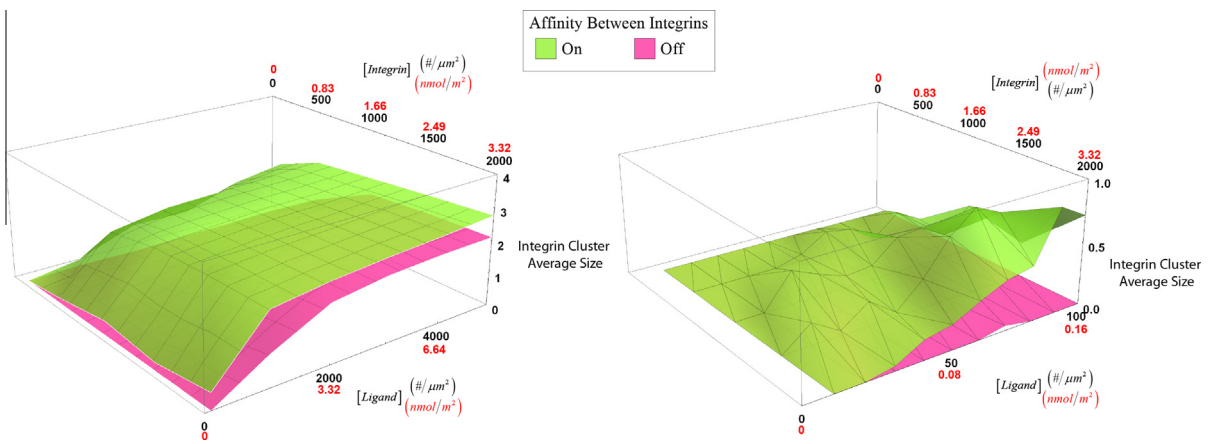

Fig. 11. Effect of homology on integrin clusters when ligands diffuse in volume 3D. Many ligands like antigens and hormones are soluble and free to diffuse in the volume. Surfaces present the results for two conditions: first, when there is affinity between integrins (green surface) and second, when there is no interaction between integrins (red surface). (For interpretation of the references to colour in this figure legend, the reader is referred to the web version of this article.)

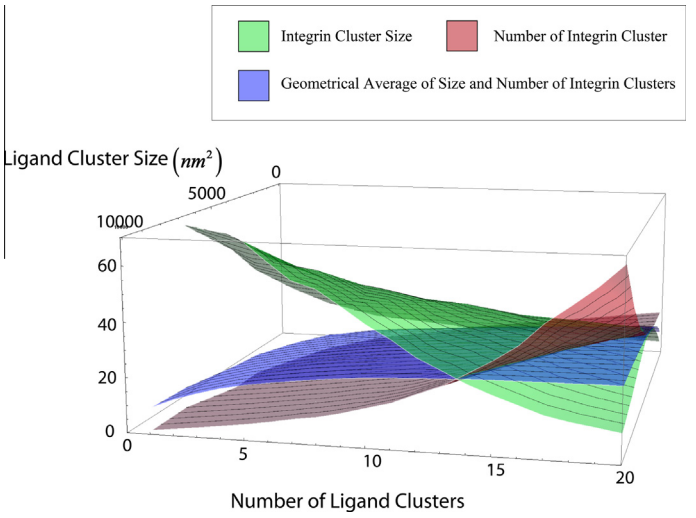

Fig. 12. Relation between the number and size of integrin clusters. There is an inverse relation between the number and the size of integrin clusters. We can assume that the geometrical average of size and number of clusters is constant; however, there is a reduction in the geometrical average at low numbers of ligand islands.

clustering is negligible. It can be speculated that at situations such as ligand-receptors, the role of homology is dominant. On the other hand, for interactions of cell adhesion, clustering ligand play a dominant role on integrin clustering. We know that integrin clustering is critical for intimal formation of focal complexes. However, this process is very dependent on ligand clustering and finally clustering ligand from the outside of the cell controls the initial integrin clustering property. Cells can rearrange the ligand distribution and possibly in this manner, indirectly control the integrin clustering and stimulate the initial state of cell adhesions.

4. Conclusion

We have developed an agent-based model of integrin clustering. By investigating the ligand organization, we found that in order to achieve the largest size of integrin clusters, the size of the ligand islands must be large and the number of islands must be low. In addition, our results showed that with a random distribution of ligand, with a sufficiently high concentration, the average size of integrin clusters is independent of ligand concentration and remains nearly constant. We demonstrated that increasing affinity between homo-subunits enhances the size of integrin clusters. The highest impact of affinity on integrin clustering happens when the ligand and integrin concentrations are near low and high, respectively. Additionally, we demonstrated that in order to serve a significant role in integrin clustering, the affinity between homo subunits should be higher than reported, *in vitro* values. However, it appears that when the ligands are immobilized, the effect of homo-subunit affinity on the integrin clustering is lower compared with that of the ligand clustering. Another major point highlighted in our results is the variation and dependency of effective affinity on concentration of ligands and integrins. The minimum value of effective affinity happens at minimum ligand and maximum integrin concentrations. At higher ligand concentrations, the effective affinity is independent of the integrin concentration. However, at low concentrations of ligands, the number of integrins has a negative effect on it. In general, the concentration of ligands has a positive effect on the effective affinity. By changing the membrane crowdedness, we observed that with a random distribution of ligands, the effect of inert particles in the system (representing higher crowdedness) is more pronounced compared to a clustered ligand distribution. In addition, the results of studying the affinity between integrins and ligands showed that at all integrin concentrations, the size of the integrin clusters increases when the affinity between ligand and integrin increases. It seems that at low concentration of soluble (mobilized in 3D) ligands, the role of integrin–integrin interactions on integrin clustering is vital and without such interactions integrin clustering is negligible.

In closing, it must be remarked that the ABM simulation allows for exploring the short- and long-term consequences of a wide range of variations in input parameters, underlying assumptions, or any general scenario changes. One of the advantages of simulation is easily addressing of the "what if?" questions. ABM simulation makes it possible to answer many such questions even beyond what happens in reality or when testing in the real world is too expensive or too time-consuming or simply impossible (due e.g. to lack of experimental infrastructures). But, of course, the reliability of results depends completely on the type of the model, the underlying phenomena and the simplifications made in the model. For this reason, in most of our presented results we have attemped to elucidate the mechanism underlying the phenomena and have strived to explain a reasonable physical meaning for the numerical patterns. When possible, we have included experimental evidence to support our results. In other cases where experimental evidence was unavailable, we hope that our results will

inspire experimental investigations to further exmaine these findings. Nonetheless, these results could help us to better understand the role of certain factors in integrin clustering with the hope to further explore the underlying mechanisms and relationships among different elements involved in this system.

Acknowledgment

The authors gratefully acknowledge fruitful discussions with and technical assistance by Mohammad Azimi, Mehrdad Mehrbod and the rest of Molecular Cell Biomechanics Laboratory. Financial support by an National Science Foundation CAREER award (CBET-0955291) is gratefully acknowledged.

References

[1] J.A. Askari, P.A. Buckley, A.P. Mould, M.J. Humphries, Linking integrin conformation to function, J. Cell Sci. 122 (2009) 165–170.
[2] A. Banno, M.H. Ginsberg, Integrin activation, Biochem. Soc. Trans. 36 (2008) 229–234.
[3] J.S. Bennett, B.W. Berger, P.C. Billings, The structure and function of platelet integrins, J. Thromb. Haemost. 7 (1) (2009) 200–205.
[4] C.J. Brinkerhoff, J.J. Linderman, Integrin dimerization and ligand organization: key components in integrin clustering for cell adhesion, Tissue Eng. 11 (2005) 865–876.
[5] C.J. Brinkerhoff, P.J. Woolf, J.J. Linderman, Monte Carlo simulations of receptor dynamics: insights into cell signaling, J. Mol. Histol. 35 (2004) 667–677.
[6] W.A. Comisar, N.H. Kazmers, D.J. Mooney, J.J. Linderman, Engineering RGD nanopatterned hydrogels to control preosteoblast behavior: a combined computational and experimental approach, Biomaterials 28 (2007) 4409–4417.
[7] M. Gao, K. Schulten, Integrin activation in vivo and in silico, Structure 12 (2004) 2096–2098.
[8] F.G. Giancotti, E. Ruoslahti, Transduction – integrin signaling, Science 285 (1999) 1028–1032.
[9] W.H. Goldmann, Kinetic determination of focal adhesion protein formation, Biochem. Biophys. Res. Commun. 271 (2000) 553–557.
[10] D.S. Harburger, D.A. Calderwood, Integrin signalling at a glance, J. Cell Sci. 122 (2009) 159–163.
[11] T. Hato, N. Pampori, S.J. Shattil, Complementary roles for receptor clustering and conformational change in the adhesive and signaling functions of integrin alphaIIb beta3, J. Cell Biol. 141 (1998) 1685–1695.
[12] D. Iber, I.D. Campbell, Integrin activation – the importance of a positive feedback, Bull. Math. Biol. 68 (2006) 945–956.
[13] D.J. Irvine, K.A. Hue, A.M. Mayes, L.G. Griffith, Simulations of cell-surface integrin binding to nanoscale-clustered adhesion ligands, Biophys. J. 82 (2002) 120–132.
[14] M. Kato, M. Mrksich, Using model substrates to study the dependence of focal adhesion formation on the affinity of integrin–ligand complexes, Biochemistry 43 (2004) 2699–2707.
[15] K. Kawakami, H. Tatsumi, M. Sokabe, Dynamics of integrin clustering at focal contacts of endothelial cells studied by multimode imaging microscopy, J. Cell Sci. 114 (2001) 3125–3135.
[16] M. Kim, C.V. Carman, T.A. Springer, Bidirectional transmembrane signaling by cytoplasmic domain separation in integrins, Science 301 (2003) 1720–1725.
[17] L.Y. Koo, D.J. Irvine, A.M. Mayes, D.A. Lauffenburger, L.G. Griffith, Co-regulation of cell adhesion by nanoscale RGD organization and mechanical stimulus, J. Cell Sci. 115 (2002) 1423–1433.
[18] E. Laplantine, P. Maurer, L. Vallar, J. Eble, M. Paulsson, P. Bruckner, N. Kieffer, M. Aumailley, The integrin beta1 subunit cytoplasmic tail forms oligomers: a potential role in beta1 integrin clustering, Biol. Cell 94 (2002) 375–387.
[19] D.J. Leahy, New light on the integrin switch, Structure 10 (2002) 1152–1154.
[20] R. Li, C.R. Babu, J.D. Lear, A.J. Wand, J.S. Bennett, W.F. DeGrado, Oligomerization of the integrin alphaIIbbeta3: roles of the transmembrane and cytoplasmic domains, Proc. Nat. Acad. Sci. USA 98 (2001) 12462–12467.
[21] R. Li, J.S. Bennett, W.F. Degrado, Structural basis for integrin alphaIIbbeta3 clustering, Biochem. Soc. Trans. 32 (2004) 412–415.
[22] R. Li, N. Mitra, H. Gratkowski, G. Vilaire, R. Litvinov, C. Nagasami, J.W. Weisel, J.D. Lear, W.F. DeGrado, J.S. Bennett, Activation of integrin alphaIIbbeta3 by modulation of transmembrane helix associations, Science 300 (2003) 795–798.
[23] B.H. Luo, C.V. Carman, T.A. Springer, Structural basis of integrin regulation and signaling, Ann. Rev. Immunol. 25 (2007) 619–647.
[24] B.H. Luo, C.V. Carman, J. Takagi, T.A. Springer, Disrupting integrin transmembrane domain heterodimerization increases ligand binding affinity, not valency or clustering, Proc. Nat. Acad. Sci. USA 102 (2005) 3679–3684.
[25] G. Maheshwari, G. Brown, D.A. Lauffenburger, A. Wells, L.G. Griffith, Cell adhesion and motility depend on nanoscale RGD clustering, J. Cell Sci. 113 (10) (2000) 1677–1686.
[26] S.P. Mirza, B.D. Halligan, A.S. Greene, M. Olivier, Improved method for the analysis of membrane proteins by mass spectrometry, Physiol Genomics 30 (1) (2007) 89–94.
[27] M.J. Paszek, D. Boettiger, V.M. Weaver, D.A. Hammer, Integrin clustering is driven by mechanical resistance from the glycocalyx and the substrate, Plos Comput. Biol. 5 (2009).
[28] M.D. Pierschbacher, E. Ruoslahti, Cell attachment activity of fibronectin can be duplicated by small synthetic fragments of the molecule, Nature 309 (1984) 30–33.
[29] J.A. Rowley, Z.X. Sun, D. Goldman, D.J. Mooney, Biomaterials to spatially regulate cell fate, Adv. Mater. 14 (2002) 886–889.
[30] E. Ruoslahti, RGD and other recognition sequences for integrins, Ann. Rev. Cell Dev. Biol. 12 (1996) 697–715.
[31] O. Thoumine, J.J. Meister, A probabilistic model for ligand-cytoskeleton transmembrane adhesion: predicting the behavior of microspheres on the surface of migrating cells, J. Theor. Biol. 204 (2000) 381–392.
[32] J. Vitte, A.M. Benoliel, P. Eymeric, P. Bongrand, A. Pierres, Beta-1 integrin-mediated adhesion may be initiated by multiple incomplete bonds, thus accounting for the functional importance of receptor clustering, Biophys. J. 86 (2004) 4059–4074.
[33] W. Wang, B.H. Luo, Structural basis of integrin transmembrane activation, J. Cell Biochem. 109 (2010) 447–452.
[34] E.S. Welf, U.P. Naik, B.A. Ogunnaike, Regulation of integrin clustering: models and experiments, spotlight talk, in: The Second qBio Conference on Cellular Information Processing Santa Fe, NM, 2008.
[35] S. Wiesner, A. Lange, R. Fassler, Local call: from integrins to actin assembly, Trends Cell Biol 16 (2006) 327–329.
[36] P.J. Woolf, J.J. Linderman, Self organization of membrane proteins via dimerization, Biophys. Chem. 104 (2003) 217–227.